Journal of the European Ceramic Society 22 (2002) 2231–2241

www.elsevier.com/locate/jeurceramsoc

Thermal removal of multicomponent binder from ceramic injection mouldings

M. Trunec*, J. Cihlar

Department of Ceramics, Brno University of Technology, Technická 2, 616 69 Brno, Czech Republic

Received 1 August 2001; received in revised form 14 December 2001; accepted 28 December 2001

Abstract

Thermal removal of polymer binder containing low-molecular-weight components from ceramic injection mouldings was studied. The effect of the shape and size of bodies on the process of binder removal was examined. Evaporation of low-molecular-weight components represented the most important process at the beginning of binder removal. It was found that a bed of activated carbon speed up removal of low-molecular-weight components. The mechanism of binder removal in a bed of activated carbon was described. Binder redistribution and evolution of porosity in the body during binder removal was investigated. A high rate of binder removal resulted in non-uniform binder distribution in the body. The formation of defects due to non-uniform binder removal was described and requirements for their elimination were proposed.

Keywords: Al_2O_3; Binder removal; Defects; Injection moulding; Porosity

1. Introduction

Binder removal represents a difficult step not only in the method of ceramic injection moulding but also in the other methods of ceramic plastic shaping.[1] When using fine ceramic powders and preparing large bodies the removal of binder is even more difficult.[1] In most cases, binder removal puts limits on the size and shape complexity of injection moulded parts since with large cross section of the body it is not possible to remove the binder in an acceptable period of time and without defects.[2] Although a number of advanced methods for binder removal have been developed (supercritical debinding,[3] catalytic debinding,[4] solvent debinding[5]) that speed up this process and make it more effective, thermal removal of binder remains, thanks to its universality and simplicity, the most widely used and up to now irreplaceable method. The thermoplastic binders currently used for ceramic injection moulding are made up of several components[6] and their thermal removal from ceramic green bodies is based on three mechanisms.[7] They are evaporation, thermal degradation and oxidative degradation. Low-molecular-weight components are not subject to chain scission and the weight loss is the result of these components diffusing towards the body surface or to the liquid–vapour interface, and then evaporating. Binder components of higher molecular weight are thermally degraded. Thermal degradation proceeds uniformly over the whole volume of polymer phase. The products of degradation also diffuse towards the body surface or towards the liquid–vapour interface, where they evaporate. The presence of oxygen in the atmosphere during thermal extraction entails in addition to thermal degradation also oxidative degradation of polymer binder, which proceeds from the surface to the centre of the body and is limited by the diffusion of oxygen into the binder or by the diffusion of the products of degradation back to the surface and their evaporation.[8] If the body being extracted is surrounded with an appropriate porous medium (powder bed, porous substrate), then yet another mechanism of binder removal can be found acting, in which capillary forces make the binder flow from the body and extracted into the surrounding medium.[9] If the local concentration of the volatile component (low-molecular-weight components of the binder or degradation products of polymer components) exceeds the critical concentration value for the given temperature, this component starts boiling, i.e. there is spontaneous gas evolution and bubble formation in the body volume.[10] The critical component

* Corresponding author. Tel.: +420-5-4114-3339; fax: +420-5-4114-3202.

E-mail address: trunec@zam.fme.vutbr.cz (M. Trunec).

0955-2219/02/$ - see front matter
PII: S0955-2219(02)00015-8

concentration appears when the saturated vapour pressure of volatile component in the binder exceeds the pressure of ambient atmosphere. Defects due to the boiling in the binder-saturated moulding structure are considered to be the greatest problem of thermal removal of binder. A number of authors have modelled binder removal from the viewpoint of critical concentration of volatile component on simplified polymer-ceramic powder systems.[10–13] Regarded as the controlling step in these cases was the diffusion of volatile degradation products through the liquid polymer towards the body surface or the binder–atmosphere interface. They did not regard evaporation as the limiting step in binder removal and assumed that for extraction analysis the zero concentration of volatile component on body surface or at the binder–atmosphere interface can be considered. Angermann and Van Der Biest[14] describing experimental removal of multicomponent binder also regarded the diffusion of volatile component in the binder as the controlling step in binder removal. However, this assumption should be always confirmed by an experiment. An important factor in the analysis of binder removal is whether the binder is capable of being transported due to capillary forces acting in ceramic powder compacts. Shaw and Edirisinghe[15] observed that the nascent porosity was lower than it would correspond to binder losses. The reason was the shrinkage of the body and binder migration in the extracted body. Cima and Lewis[16–18] showed in their works that binder redistribution due to capillary forces during the removal of the volatile component led to the appearance of non-planar liquid–vapour interface. This reduced the diffusion path of volatile components and thus greatly speeded up the transport of volatile components towards the phase interface, where the components evaporated. Lewis et al.[19] performed a computer simulation of porosity appearing during the removal of two-component binder with a low-molecular-weight (volatile) and a polymer (non-volatile) component at temperatures below the temperature of polymer component degradation. The simulation assumed unrestricted binder redistribution in the body due to capillary forces. The simulation results confirmed the validity of the model of non-planar liquid–vapour interface and penetrating porosity. The simulation also showed quantitatively the inadequateness of models with non-intrusion interface or with planar interface advancing into the body centre (shrinking core model). Bandyopadhyay and French[20] reported that the redistribution of ceramic particles due to the flow of binder from the body into the surrounding medium led in large mouldings such as turbine rotors to the appearance of cracks.

The aim of the present work has been to describe the events in the initial stage of removing the multicomponent binder containing low-molecular-weight components from fine powder mouldings, and to establish in what way and to what extent the binder losses in this region can be affected.

2. Experimental

2.1. Materials and the preparation of injection mouldings

For the preparation of ceramic injection mouldings, alumina (RC-HP DBM, Malakoff Industries, USA) was used, particle size (d_{50}) 0.57 μm, specific surface 7.5 $m^2 g^{-1}$. Thermoplastic binder contained 50 wt.% of ethylene-vinyl acetate (EVA) copolymer (Elvax 250, Du Pont de Nemours, USA), 34 wt.% of paraffin wax (52/54, Koramo, CR) and 16 wt.% of stearic acid (1.00671, Merck, Germany). At 130 °C and a shear rate of 1−10 s^{-1} the binder viscosity was 18 Pa s. The ceramic powder loading in the suspension was 86 wt.% (60 vol.%). Ceramic suspension for injection moulding was prepared by mixing the ceramic powder and binder in a heated kneader (HKD 2.5, IKA-Werk, Germany). Ceramic injection mouldings in the shape of discs (diameter 42 mm. thickness 2.1, 3, 4.4 and 7.9 mm), cylinders (diameter 5.9 mm, length 60 mm) and balls (diameter 15 mm) were prepared on an injection moulding machine (Allrounder 220M, Arburg, Germany). For a comparison of the binder removal process with injected bodies ceramic granules were prepared with a large surface area to volume ratio. Ceramic granules were obtained by crushing and sieving the ceramic feedstock and had an average particle size of 0.9 mm.

2.2. Binder removal and evaluation methods

Binder removal at a constant rate of heating took place at a temperature increase of 10 °C h^{-1} and a nitrogen rate of flow of 3.3 $cm^3 s^{-1}$. During extraction, ceramic injection mouldings were loosely suspended so that gas could flow uniformly around the whole body. The extraction device enabled continual recording of the weight of extracted bodies. The device was described in detail in a previous paper.[21] The number of extracted bodies in each experiment was chosen such that the total surface area of all bodies was ca 15 000−16 000 mm^2 (except for a debinding experiment with 10 discs of total surface area ca 30 000 mm^2). To determine the weight losses of pure binder and EVA copolymer, foils of 0.3 mm in thickness and 60 mm in diameter were prepared. The foils were prepared by pressing the binder or the EVA copolymer between heated metal plates. The foils as well as the ceramic granules were placed on the bottom of four glass dishes, suspended in the extraction device and exposed to the same extraction cycle as ceramic injection mouldings. Binder removal

under isothermal conditions took place at a temperature of 130 °C and a nitrogen rate of flow of 6 $cm^3\ s^{-1}$ in a muffle furnace (312S, Linn High Therm, Germany). In the course of binder removal the bodies were placed in powder beds and, for comparison, also left free, without a powder bed. The bodies were placed such that the powder layer embedding the body was 10–15 mm thick. Granular activated carbon, powdered activated carbon and coarse alumina were used for powder beds. Granular carbon (GA-1, SLZ, Slovakia) had particles of 1–2.8 mm in size and specific surface larger than 1000 $m^2\ g^{-1}$. Powdered carbon was prepared by milling granular carbon in a ball mill. The size of particles in the powder obtained was $d_{50} = 0.85$ μm. The coarse fused alumina (white corundum, Carborundum Electrit, CR) had particles of 0.6 mm in size and specific surface area below 1 $m^2\ g^{-1}$.

Weight losses of bodies during isothermal binder removal were determined by weighing before and after extraction, always for three bodies. Shrinkage was determined by measuring body dimensions before and after binder removal, always at room temperature. Shrinkage determined in this way did not reflect temperature expansion of binder and corresponded to binder losses and permanent redistribution of ceramic particles. The distribution of residual binder in a disc of 4.4 mm in thickness after partial extraction was ascertained by ashing experiments on layers removed gradually from the body. The layers were removed by lathing in axial as well as radial direction. The extent of open porosity was determined by alcohol stain penetration at normal pressure. The bodies were soaked in alcohol stain for 48 h. After drying, optical microscope observation of body fractures revealed the depth of stain penetration, which gave the extent of open porosity.

3. Results and discussion

3.1. Evaporation and degradation of pure binder and EVA copolymer

The graph in Fig. 1 shows the change in weight of the 0.3 mm thick foil of binder or pure EVA copolymer in dependence on temperature at a heating rate of 10 °C h^{-1}. The binder evaporated in two distinct temperature regions. The first region was in the temperature range from 130 to 310 °C. In this region some 60 wt.% of binder was removed. In the second region the binder weight diminished faster than in the first region and in the range from 380 to 440 °C most of the remaining 40 wt.% of binder was removed. At 450 °C all the binder was completely removed. The degradation of EVA copolymer took place in two stages. In the first stage 20 wt.% of copolymer was removed in the 250–310 °C range. Below 250 °C there were no changes in weight. The weight loss in the first stage of EVA copolymer degradation was due to the elimination of side acetate groups ($-OCOCH_3$) in vinyl acetate units. Hrdina et al.[22] claimed that at this stage the sole degradation product was acetic acid (CH_3COOH) with the boiling point at 118 °C. If we consider a 28 wt.% proportion of vinyl-acetate of the grade of the EVA copolymer used, then the 20 wt.% loss established for the first stage just corresponded to the removal of all acetate groups. The removal of side groups gave rise to double bonds in the polymer so that the remaining polymer could be regarded as an ethylene-acetylene copolymer.[22] This copolymer degraded by chain scission at higher temperatures (380–440 °C). It follows from a comparison of the curves mentioned above that all the binder losses up to 250 °C can be regarded as evaporation of low-molecular-weight binder components, i.e. paraffin and stearic acid. The binder loss up to 250 °C represented some 44 wt.% while the total proportion of low-molecular-weight components in the binder was 50 wt.%. Another 16 wt.% of binder removed in the first temperature region (130–310 °C) corresponded to the remaining low-molecular-weight components in the binder (6 wt.%) and the acetate groups eliminated from the EVA copolymer (10 wt.%). Since the boiling point of paraffin and stearic acid is above 310 °C, acetic acid was the only component that could boil at a temperature up to 310 °C. The degradation product formed, acetic acid, diffused as dissolved gas towards the binder–atmosphere interface, where it evaporated. In the case that the critical concentration of acetic acid in the binder is exceeded, boiling sets in, i.e. evolution of gas phase throughout the whole volume of liquid binder. Hrdina et al.[23] found out in experiments that already a small amount of degraded polymer led to bubbles formation in the molten polymer. The first weight losses during thermal degradation of the EVA copolymer (Fig. 1),

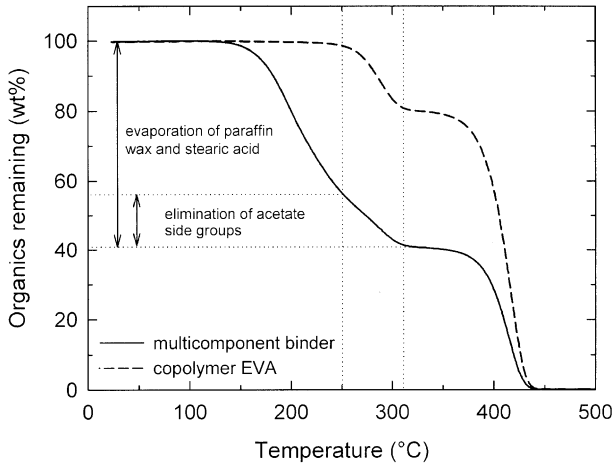

Fig. 1. Weight loss versus temperature for multicomponent binder and copolymer ethylene–vinyl acetate during heating at a rate of 10 °C h^{-1}.

which signal the appearance and evaporation of acetic acid, occurred at 250 °C. This temperature can thus be reliably regarded as a safe estimate of critical temperature for the appearance of defects due to spontaneous boiling throughout the whole volume of ceramic bodies. Hence it follows for binder removal from ceramic injection mouldings that it is necessary to achieve in the whole body the most developed open porosity possible before the temperature of 250 °C is reached. Open porosity makes it possible to eliminate the danger of degradation products boiling inside the body, because by shortening the diffusion length to the liquid binder–vapour interface and subsequent evaporation in an open porous structure, the concentration of degradation products in liquid binder is reduced more quickly.

3.2. Binder removal from ceramic injection mouldings at constant heating rate

The graph in Fig. 2 shows the temperature dependence of binder content in ceramic discs of varying thickness during binder removal at a heating rate of 10 °C h^{-1}. In Fig. 3 this comparison is shown for ceramic injection mouldings of different shapes. Similar to the pure binder, the weight in ceramic green bodies also diminished in two pronounced steps. Differences between individual bodies were found primarily in the first region of binder removal (130–310 °C). With falling ratio of surface area to volume of the body (S/V) the removal of binder was shifted to higher temperatures. The weight loss of binder in fine granules of ceramic mixture (the highest S/V ratio) had a course markedly different from that of other bodies and was close to the course of weight losses of pure binder. The second temperature region of binder removal was in all bodies almost identical and was similar to the weight changes of pure binder. There was found no porosity in the injection mouldings below 220 °C. First traces of porosity could be found in disc of 2.1 mm in thickness at 250 °C.

The number of bodies and the flow of surrounding atmosphere in the extraction device influenced the weight changes during binder removal (see Fig. 4). An increase in the number of bodies in the extraction device resulted in the curve of weight losses being only slightly shifted towards higher temperatures at the beginning of extraction. Increasing the nitrogen rate of flow from 3.3 to 16.7 cm^3 s^{-1} however led to a considerably higher extraction rate, i.e. shifting the curve of weight losses towards lower temperatures. A similar effect of the number of bodies and gas flow during extraction was also encountered in the other types of body, even in the case of pure binder.

It follows from the above results that the evaporation of low-molecular-weight components was the decisive process at the beginning of binder removal. The rate of evaporation, V_E (kg m^{-2} s^{-1}), is determined according to the relation[24]

$$V_E = k \cdot (p_v - p_a) \quad (1)$$

where p_v is the pressure of saturated vapours of volatile (low-molecular-weight) component over the binder (Pa), p_a is the partial pressure of this component in surrounding atmosphere (Pa), and k is the surface mass transfer coefficient (m^{-1} s) dependent on temperature, geometry of the body and the flow of surrounding atmosphere. During evaporation there appears on the body surface a stagnant boundary layer of vapour which controls the vapour transport.[24] Above this layer is already homogeneous atmosphere with the partial pressure of evaporated component equal to p_a. Changes

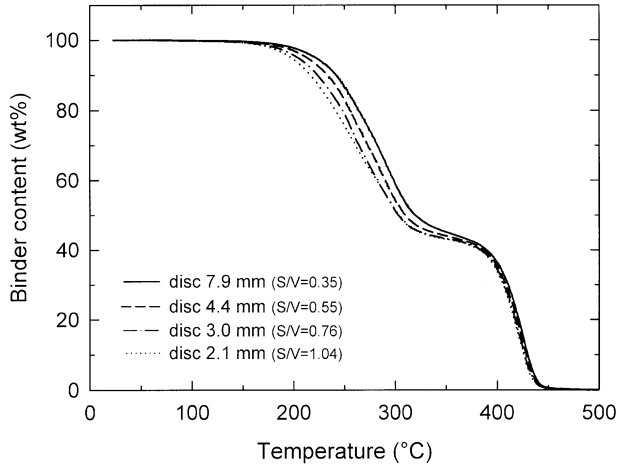

Fig. 2. Binder content in various discs versus temperature during debinding at a heating rate of 10 °C h^{-1}. The surface-area to volume ratio (S/V, in units of mm^{-1}) for each specimen is indicated in parentheses in the figure.

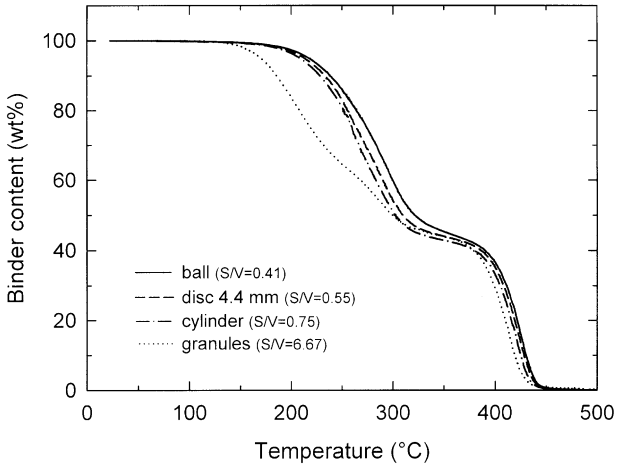

Fig. 3. Binder content in specimens of different shapes versus temperature during debinding at a heating rate of 10 °C h^{-1}. The surface-area to volume ratio (S/V, in units of mm^{-1}) for each specimen is indicated in parentheses in the figure.

in the number of bodies and in the rate of gas flow led to changes in the partial pressure of vapours of paraffin, stearic acid or acetic acid in the surrounding atmosphere, and to affecting the stagnant boundary layer (changes in thickness and concentration). This entailed a change in the rate of evaporation. A comparison of the rate of binder removal from bodies of different shapes relative to unit surface area (Fig. 5) shows that at the beginning all losses copy the same curve (as the mechanism of evaporation assumes) and only with increasing temperature did they gradually deviate from it. The gradual deviation from the common curve in individual bodies was due to the different decrease of paraffin and stearic acid in the binder (in dependence on the S/V ratio) and consequently to the different activities of volatile components in the binder. The activity of volatile component determines the pressure of saturated vapours above the polymer solution and thus also the rate of evaporation. It should be noted that the initial agreement in the rate of removal mentioned above was reached only in the case that the total area of extracted bodies was always identical.

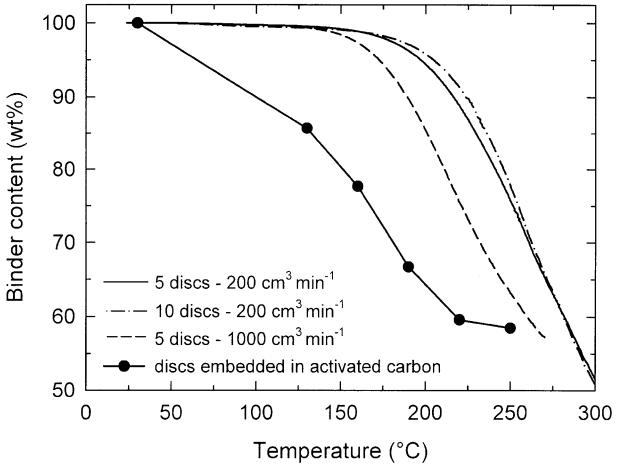

Fig. 4. Binder content in discs (thickness 2.1 mm) versus temperature during debinding at a heating rate of 10 °C h^{-1} with different gas flow rate and different number of specimens in the debinding furnace. Binder content in discs (thickness 2.1 mm) embedded in powdered carbon is also shown for comparison.

For comparison, Fig. 4 gives the plot of weight losses established for binder removal from discs embedded in activated carbon. In particular in the region of lower temperatures the losses were much higher than was the case of freely placed bodies, even if the flow of surrounding atmosphere was intensive. In a previous paper Trunec and Cihlar[25] showed that microporous particles of activated carbon speed up binder removal due to their high specific surface but an exact mechanism was not clearly defined. The mechanism of binder removal in a bed of activated carbon is suggested and discussed in detail below.

3.3. Isothermal binder removal from ceramic injection mouldings

3.3.1. Mechanism of binder removal in activated carbon bed

The temperature chosen for isothermal binder removal, 130 °C, was low enough to prevent the low-molecular-weight components (paraffin and stearic acid) from boiling and to make the degradation of polymer component negligible even with a long holding time at this temperature. For all shapes of bodies the highest binder losses were established for the extraction in a bed of powdered carbon (Figs. 6–8). High losses were also established for the extraction in granular carbon. It has been shown in the previous paper[25] that the published models of capillary extraction cannot explain the high binder losses in a bed of activated carbon. The high binder losses in a bed of granular carbon confirmed that capillary forces were not decisive in removing the binder

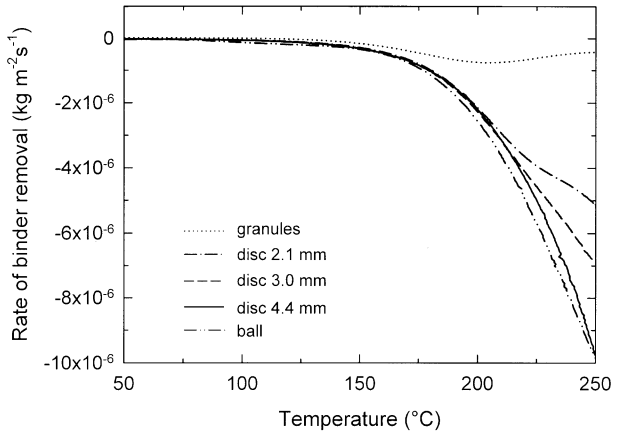

Fig. 5. Rate of binder removal per unit area of surface of different specimens as a function of temperature during debinding at a heating rate of 10 °C h^{-1}.

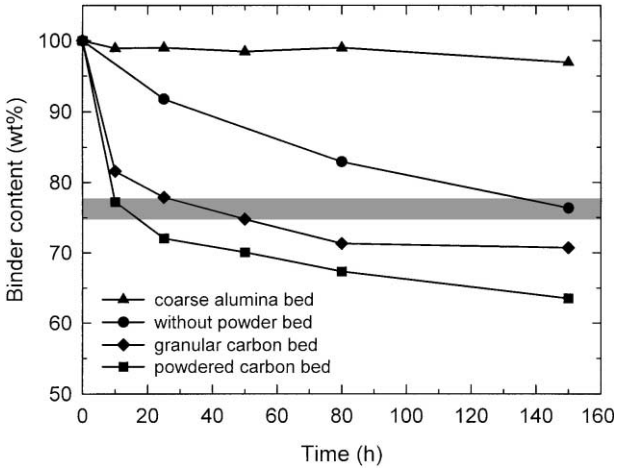

Fig. 6. Binder content in discs (thickness 2.1 mm) versus time during isothermal debinding in various powder beds and without a powder bed at 130 °C.

from ceramic green bodies in activated carbon since the large granules of carbon (1–2.8 mm) did not form small interparticle pores necessary for capillary extraction of liquid binder. Binder removal must therefore have taken place in the gaseous phase by evaporation of low-molecular-weight components. Evaporated binder diffused towards the surface of carbon particles, where it adsorbed on the surface. The decisive factor was thus the large specific surface area of activated carbon formed by internal porosity of carbon particles.[25] If binder vapours did not adsorb on the surface of activated carbon, the vapours would have to diffuse into surrounding environment through the bed and, consequently, the partial pressure at the liquid binder–atmosphere interface would increase and evaporation would grow slower. This is confirmed by the results obtained in extraction in a bed of coarse alumina. After an extraction of 150 h the binder losses established for bodies placed in coarse alumina were less than 3.5 wt.%. Large dense particles of alumina bed did not enable capillary extraction of liquid binder and the small specific surface area of particles (<1 m^2 g^{-1}) did not enable adsorption of a greater amount of binder. Evaporation was made difficult and binder losses were negligible even in comparison with binder losses in freely placed bodies. In freely placed bodies, evaporation was facilitated by vapours of low-molecular-weight binder components being removed from the surface of bodies by the flow of surrounding atmosphere. An additional experiment was performed to confirm the adsorption of binder vapours on carbon surface. An open container with granular activated carbon and an embedded injection moulded disc was heated up to 250 °C and cooled down. After cooling the weight of the container was almost the same as before heating although the disc showed a 40 wt.% binder loss. We can conclude that the removed binder was now stored in the carbon bed. If we suppose a negligible capillary flow of liquid binder from the body to the bed then the adsorption of binder vapours on the carbon surface is the most probable explanation of this phenomenon.

Activated powdered carbon was obtained by milling granules of activated carbon. The related change in the specific surface area of activated carbon was negligible. The cause of the higher binder losses during extraction in powdered carbon compared to extraction in granular carbon can be sought in the reduced diffusion path of the binder vapours to the surface of carbon particles resulting from a closer contact between the particles of the milled carbon and the surface of the extracted body. This influenced the stagnant boundary layer of vapours of low-molecular-weight components at the phase interface and led to a higher rate of evaporation. Activated carbon thus accelerates binder removal thanks to a higher rate of binder evaporation, similar to the intensive gas flow in the case of freely placed bodies.

3.3.2. Binder redistribution and porosity evolution

The grey area in the graphs in Figs. 6–8 represents the region of binder loss in the course of which partial porosity was observed in the specimens, that is to say the specimens were non-porous above this region (without open porosity) while below this region open porosity penetrated the whole body. With the binder loss exceeding 25 wt.%, open porosity could be encountered in the whole volume of all the bodies examined. The region of binder loss at which the bodies exhibited partial porosity was narrow, above all in the case of the thinnest discs (of 2.1 mm in thickness). The narrow region of partial porosity meant that during extraction the binder was uniformly redistributed in the body, i.e. the binder from the centre of the body complemented the binder evaporating from the body surface. With discs of 4.4 mm in thickness the region of binder loss at

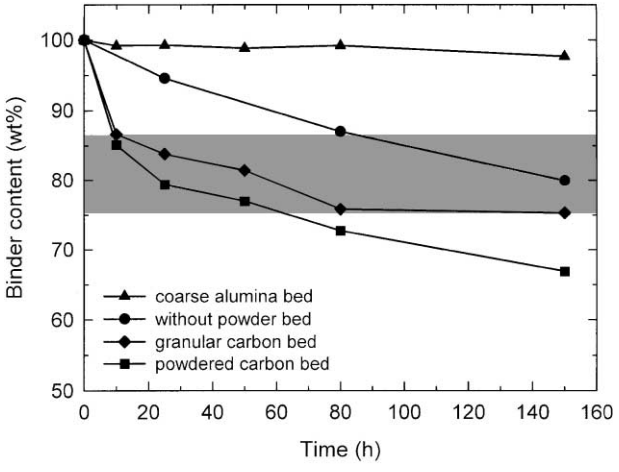

Fig. 7. Binder content in discs (thickness 4.4 mm) versus time during isothermal debinding in various powder beds and without a powder bed at 130 °C.

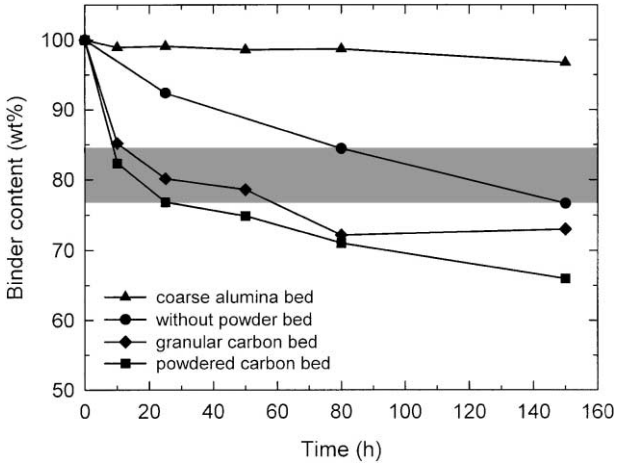

Fig. 8. Binder content in cylinders versus time during isothermal debinding in various powder beds and without a powder bed at 130 °C.

which the bodies had partial porosity grew wider towards lower binder losses. The wider region of partial porosity meant that the transport of binder from inside the body to the surface was not fast enough, which led to formation of porosity in the surface layer and thus to inhomogeneity in binder distribution in the body. An exception was the free-extracted disc, in which even with a 20 wt.% binder loss no porous layer appeared. Thanks to the lower extraction rate the binder in this disc could be redistributed, similar to the discs with 2.1 mm thickness.

The distribution of the residual binder in the free-extracted disc of 4.4 mm in thickness was nearly uniform in both axial and radial direction during all periods of binder removal. Binder distribution in a 4.4 mm thick disc extracted in a bed of powdered carbon (Fig. 9a and b) was uniform in the axial direction only. In the radial direction, a reduction is evident of the residual binder in the surface layer in the case of shorter times of binder removal. After 150 h the distribution of binder in these bodies was again uniform.

The evolution of porosity during binder removal can be seen in Fig. 10. In discs that were extracted for 10 and 50 h in a bed of powdered carbon a transition can be seen between the porous surface layer (dark region) and the non-porous centre (light region). After 80 h of extraction, open porosity had already penetrated the whole disc. The reason for preferred porosity widening in the radial direction is not quite clear. In the course of injection, the non-spherical particles of ceramic powder probably got aligned in the direction in which the disc cavity was filled with ceramic suspension.[26] This created an oriented structure that facilitated the flow of binder in the direction of particle orientation, i.e. radial direction. This hypothesis finds support in the fact that shrinkage during sintering was also anisotropic.[27] A comparison of discs with 20 wt.% binder loss extracted either in a bed of powdered carbon or free, without a powder bed (Fig. 11) shows the difference in porosity evolution. In the free-extracted body the binder was redistributed and with a 20 wt.% binder loss there was still no open porosity. By contrast, in a disc with the same binder loss but extracted in a bed of powdered carbon, a part of the disc is already porous. The flow of binder from the disc centre was not sufficient to compensate the high binder loss on the disc surface at the beginning of extraction. This gave rise to partial porosity in the surface layer at a lower binder loss than in the case of the more slowly extracted body.

Binder loss and the appearance of porosity also affected the volume shrinkage of bodies during binder removal. Fig. 12 shows the volume shrinkage of discs 2.1 mm thick in dependence on binder loss. With decreasing binder content the disc was shrinking uniformly as the particles were coming closer to one

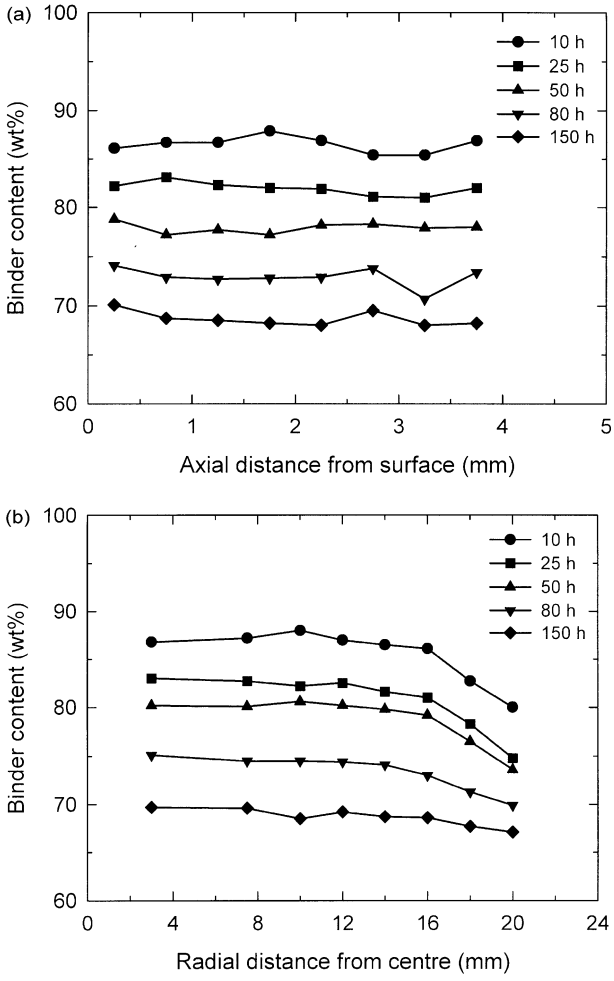

Fig. 9. Distribution of residual binder in discs (thickness 4.4 mm) after debinding in a bed of powdered activated carbon at 130 °C for different holding times; (a) in the axial direction, (b) in the radial direction.

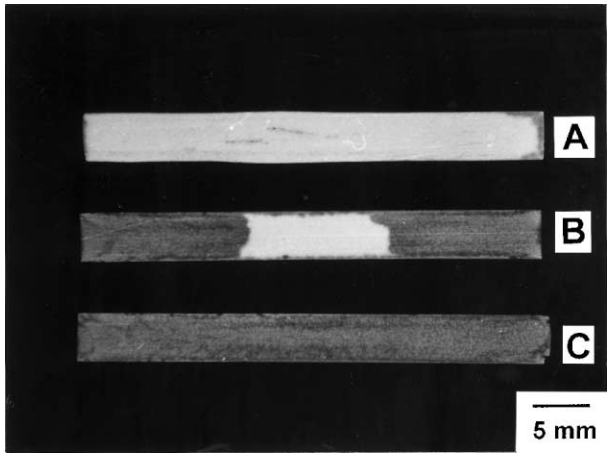

Fig. 10. Microphotograph of polished cross sections of discs (thickness 4.4 mm) debinded in a bed of powdered activated carbon at 130 °C for (A) 10 h, (B) 50 h, (C) 80 h. Binder saturated area — bright, porous area — dark.

another. The moment the particles got into mutual contact, any further movement of particles was blocked and the shrinking stopped (at a shrinkage of 7 vol.%). Any further binder loss meant the appearance of porosity. With the appearance of porosity there was a drop in the forces acting on ceramic particles. Forces induced by capillary tension decreased with porosity penetrating into the body and part of the shrinkage relaxed. Further shrinkage continued only in the region of higher binder loss, when the binder was being removed that was adsorbed on the surface of particles and prevented their total contact. When all the binder was removed, the volume shrinkage was 7.2 vol.%, i.e. only 0.2–0.3 vol.% higher than at the moment when porosity started to appear. In the disc with 4.4 mm thickness, the nature of the dependence of volume shrinkage on binder loss (Fig. 13) was different for free-extracted bodies and bodies extracted in a bed of activated carbon. The initial part of the shrinkage of the free-extracted disc copied the dependence established for the disc of 2.1 mm in thickness. In the discs extracted in activated carbon (both powdered and granular) the dependence of shrinkage on binder loss was also similar to that of 2.1 mm thick discs but the maximum shrinkage at the appearance of porosity was only 5% and was shifted to lower binder loss. Moreover, the maximum did not correspond to the exact beginning of porosity formation, it occurred inside a wider region of partial porosity. These two differences can be explained as a result of non-uniform binder removal.

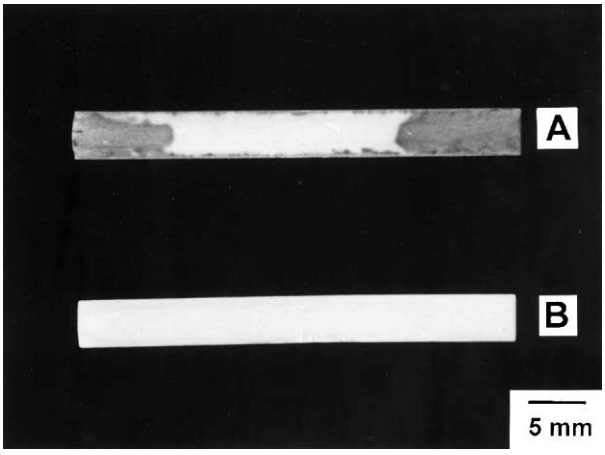

Fig. 11. Microphotograph of polished cross sections of discs (thickness 4.4 mm) debinded at 130 °C (A) in a bed of powdered activated carbon for 25 h, (B) without a powder bed for 150 h. 20 wt% of binder removed in both specimens. Binder saturated area — bright, porous area — dark.

3.4. Formation of defects

The above results have shown that a bed of activated carbon made it possible to speed up binder removal in the region below the critical temperature of defects arising due to the boiling of binder or its degradation products. At the same time it was found, however, that the high rate of binder loss in bodies with a lower S/V ratio led to inhomogeneous distribution of binder in the body. This inhomogeneity can lead to the formation of defects, as can be seen in the fracture of extracted cylinder in Fig. 14. The mechanism of the evolution of these defects can be explained as follows. At the beginning of extraction the ceramic particles are distributed uniformly and mutually separated by a binder layer. During intensive evaporation the flow of binder from the centre to the body surface is not sufficiently rapid and the surface layers shrink more than the body centre. At the moment the binder is removed also from the

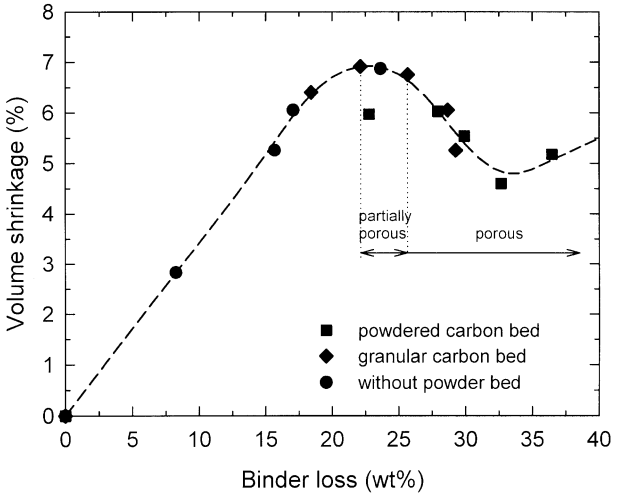

Fig. 12. Volume shrinkage of discs (thickness 2.1 mm) versus binder loss during isothermal debinding in different carbon beds and without a bed at 130 °C.

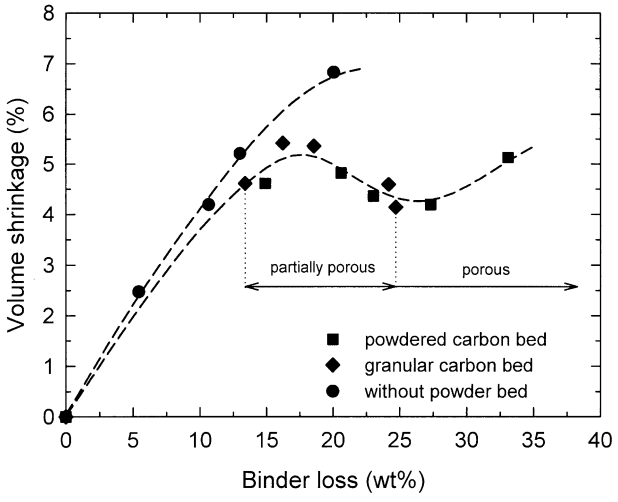

Fig. 13. Volume shrinkage of discs (thickness 4.4 mm) versus binder loss during isothermal debinding in different carbon beds and without a bed at 130 °C.

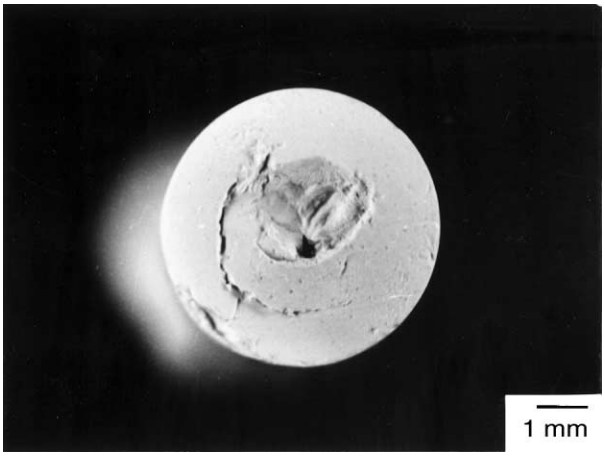

Fig. 14. Microphotograph of fracture surface of a presintered cylinder debinded at a heating rate of 10 °C h^{-1} in a bed of powdered activated carbon.

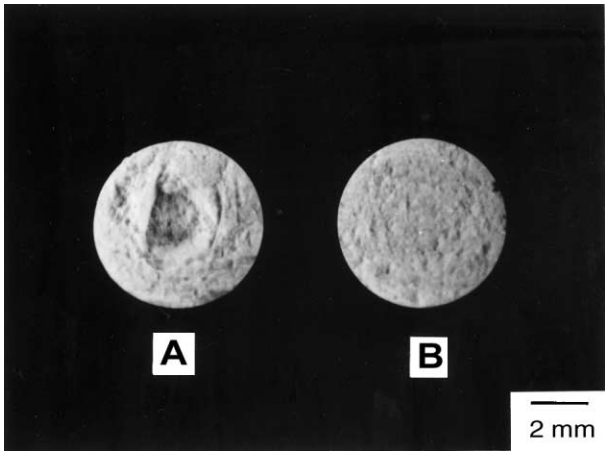

Fig. 15. Microphotograph of fracture surface of cylinders debinded in a bed of powdered activated carbon (A) to 220 °C at a heating rate of 10 °C h^{-1}, (B) to 130 °C at a heating rate of 10 °C h^{-1} with holding time of 150 h at 130 °C. 35 wt.% of binder removed in both specimens.

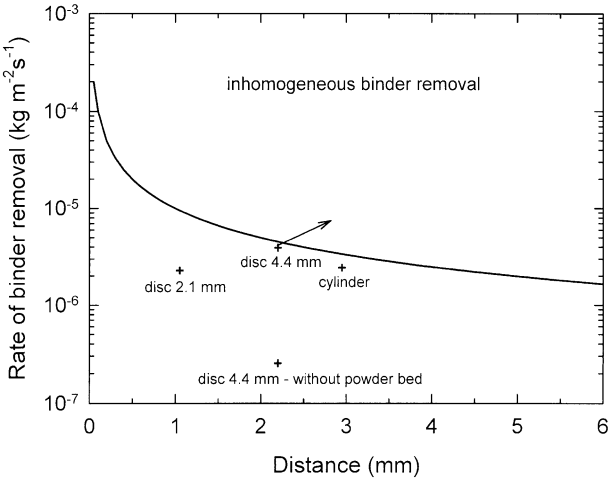

Fig. 16. Dependence of the maximum rate of binder removal on the transport distance of liquid binder at 130 °C.

body centre and the body centre starts shrinking, the solid porous surface layer prevents further shrinkage and a typical circular defect appears. Reducing the rate of binder removal at the beginning of extraction can prevent the appearance of these defects. Fig. 15 gives a comparison of the fracture structure of cylinders extracted in a bed of powdered carbon, with roughly the same binder loss (35 wt.%) but with different temperature modes. In the case of the cylinder extracted up to 220 °C at a rate of 10 °C h^{-1}, a circular defect can be seen developing in the fracture. In the cylinder extracted at a temperature of 130 °C for a period of 150 h the fracture is without any apparent defects. The reduction in the rate of binder removal, in particular at the beginning of extraction, made it possible to obtain a more homogeneous and non-defective structure.

An optimum rate of binder removal must be chosen for every body. On the assumption that capillary flow is the principal mechanism of binder redistribution in the body, it is possible to estimate the maximum rate of binder removal from the following relation derived by Cima et al.[16] for liquid flow in porous medium due to capillary forces:

$$G = \frac{d \cdot \delta \cdot \varepsilon^3 \cdot \gamma}{18 \cdot h \cdot K \cdot (1-\varepsilon)^2 \cdot v} \quad (2)$$

where G is the mass flow of binder through unit area (kg m^{-2} s^{-1}), d is the size of ceramic particles (m), δ is a factor that depends on the packing of particles, ε is the volume fraction of binder in ceramic suspension, γ is the surface energy of liquid binder (J m^{-2}), h is the transport distance (m), K is the constant given by the geometry of pores, and v is the kinematic viscosity (m^2 s^{-1}). The values used for the solution, $K=5$ and $\delta=8$, were adopted from a paper by Cima et al.[16] The volume fraction of binder was equal to 0.4. The particle size considered was 0.6 μm. The value γ was estimated on the basis of additive group contribution theory,[28] and for 130 °C it was equal to 0.021 J m^{-2}. For kinematic viscosity it holds $v=\eta/\rho$, where η is the dynamic viscosity of binder ($\eta_{130}=18$ Pa s) and ρ is the density, whose value was estimated from the densities of binder components and binder dilatation[28] ($\rho_{130}=877$ kg m^{-3}). Fig. 16 illustrates the dependence of maximum rate of binder removal on transport distance of liquid binder determined according to Eq. (2). In the region above the curve, capillary forces are no longer able to transport the binder at the required rate. For binder removal this means that with the binder loss rate in this region the binder will not be removed uniformly from the whole volume of the body. In first approximation, the distance from the centre to the surface of the body can be regarded as the transport distance. Relation (2) holds for saturated body and it would have to be corrected if porosity appears in the body. Since the maximum rate of

binder loss was established for the beginning of extraction when all pores were fully saturated, the relation given above can be used for the estimation of the critical rate of binder removal. In the graph of Fig. 16 the points are plotted that represent the maximum rate of binder removal from bodies embedded in powdered carbon at 130 °C. The values of binder removal rate for the 4.4 mm thick disc and for the cylinder were close to the boundary where homogeneous binder removal can still be expected. If we consider anisotropic binder removal in the 4.4 mm thick disc (Fig. 10), the maximum binder loss per unit area of body surface will increase and also the transport distance will be shifted to higher values (as the arrow shows in Fig. 16). Thus at the beginning of extraction, when binder removal was at its highest, the disc reached the region of inhomogeneous binder removal. This is in agreement with the widening of the region of partial porosity in the disc of 4.4 mm in thickness as compared with the 2.1 mm thickness.

4. Conclusions

Evaporation of low-molecular-weight components was identified as the decisive process at the beginning of removal of multicomponent binder from fine powder mouldings. At this stage, binder loss decreased with decreasing ratio of the surface area of the body to its volume. A bed of activated carbon provided for quicker evaporation of low-molecular-weight binder components. Binder vapours adsorbed on the large surface area of activated carbon, which reduced the boundary layer of vapours at the binder–atmosphere interface and thus enhanced evaporation. During evaporation the binder inside the body was redistributed. Binder loss was accompanied by the shrinkage of body. At the moment the movement of particles was blocked and shrinkage stopped, open porosity began to develop in the surface layer of body and moved quickly to the body centre. With the high binder loss rates the binder could not redistribute uniformly and inhomogeneous saturation of the body with binder occurred, with porous surface layer and excess binder in the body centre. Non-uniform binder removal from the body even led to the formation of cracks. To prevent from these defects it is necessary to optimize the rate of binder removal with respect to the rate of binder redistribution in a body of given shape and size.

Acknowledgements

The authors gratefully acknowledge the funding provided by the Czech Ministry of Education under grant CEZ:J22/98:262100002.

References

1. Trunec, M. and Cihlar, J., Removal of thermoplastic binders from ceramic green bodies. *Ceramics-Silikáty*, 1997, **41**, 67–80.
2. Zhang, J. G., Edirisinghe, M. J. and Evans, J. R. G., A catalogue of ceramic injection moulding defects and their causes. *Industrial Ceramics*, 1989, **9**, 72–82.
3. Chartier, T., Ferrato, M. and Baumard, J. F., Supercritical debinding of injection molded ceramics. *J. Am. Ceram. Soc.*, 1995, **78**, 1787–1792.
4. Ebenhöch, J. and ter Maat, J., Ceramic injection molding with a polyacetal based binder system. In *Advances in Powder Metallurgy and Particulate Materials,* Vol. 5*, Powder Injection Molding*. Metal Powder Industries Federation, Princeton, 1993, pp. 73–89.
5. Tsai, D. S. and Chen, W. W., Solvent debinding kinetics of alumina green bodies by powder injection molding. *Ceram. Int.*, 1995, **21**, 257–264.
6. Mutsuddy, B. C. and Ford, R. G., *Ceramic Injection Molding*. Chapman and Hall, London, 1995 66–128.
7. Shaw, H. M. and Edirisinghe, M. J., Removal of binder from ceramic bodies fabricated using plastic forming methods. *Am. Ceram. Bull.*, 1993, **72**, 94–99.
8. Wright, J. K. and Evans, J. R. G., Kinetics of oxidative degradation of ceramic injection-moulding vehicle. *J. Mater. Sci.*, 1991, **26**, 4897–4904.
9. Wright, J. K. and Evans, J. R. G., Removal of organic vehicle from moulded ceramic bodies by capillary action. *Ceram. Int.*, 1991, **17**, 79–87.
10. Calvert, P. and Cima, M., Theoretical models for binder burnout. *J. Am. Ceram. Soc.*, 1990, **73**, 575–579.
11. Evans, J. R. G., Edirisinghe, M. J., Wright, J. K. and Crank, J., On the removal of organic vehicle from moulded ceramic bodies. *Proc. Roy. Soc. Lond.*, 1991, **A432**, 321–340.
12. Oliveira, A. A. M., Kaviany, M., Hrdina, K. E. and Halloran, J. W., Mass diffusion-controlled bubbling and optimum schedule of thermal degradation of polymeric binders in molded powders. *Int. J. Heat Mass Transfer*, 1999, **42**, 3307–3329.
13. Maximenko, A. and Van Der Biest, O., Finite element modelling of binder removal from ceramic mouldings. *J. Eur. Ceram. Soc.*, 1998, **18**, 1001–1009.
14. Angermann, H. H. and Van Der Biest, O., Low temperature debinding kinetics of two-component model system. *Int. J. Powder Metall.*, 1993, **29**, 239–250.
15. Shaw, H. M. and Edirisinghe, M. J., Porosity development during removal of organic vehicle from ceramic injection mouldings. *J. Eur. Ceram. Soc.*, 1994, **13**, 135–142.
16. Cima, M. J., Lewis, J. A. and Devoe, A. D., Binder distribution in ceramic greenware during thermolysis. *J. Am. Ceram. Soc.*, 1989, **72**, 1192–1199.
17. Cima, M. J., Dudziak, M. and Lewis, J. A., Observation of poly(vinyl butyral)-dibutyl phthalate binder capillary migration. *J. Am. Ceram. Soc.*, 1989, **72**, 1087–1090.
18. Lewis, J. A. and Cima, M. J., Diffusivities of dialkyl phthalates in plasticized poly(vinyl butyral): impact on binder thermolysis. *J. Am. Ceram. Soc.*, 1990, **73**, 2702–2707.
19. Lewis, J. A. and Galler, M. A., Computer simulations of binder removal from 2-D and 3-D model particulate bodies. *J. Am. Ceram. Soc.*, 1996, **79**, 1377–1388.
20. Bandyopadhyay, G. and French, K. W., Effects of powder characteristics on injection molding and binder removal process and component fabrication. *J. Eur. Ceram. Soc.*, 1993, **11**, 23–34.
21. Trunec, M. and Cihlar, J., Thermal debinding of injection moulded ceramics. *J. Eur. Ceram. Soc.*, 1997, **17**, 203–209.
22. Hrdina, K. E., Halloran, J. W., Oliveira, A. and Kaviany, M., Chemistry of removal of ethylene vinyl acetate binders. *J. Mater. Sci.*, 1998, **33**, 2795–2803.

23. Hrdina, K. E., Halloran, J. W., Kaviany, M. and Oliveira, A., Defect formation during binder removal in ethylene vinyl acetate filled system. *J. Mater. Sci.*, 1999, **34**, 3281–3290.
24. Scherer, G. W., Theory of drying. *J. Am. Ceram. Soc.*, 1990, **73**, 3–14.
25. Trunec, M. and Cihlar, J., Effect of activated carbon bed on binder removal from ceramic injection moldings. *J. Am. Ceram. Soc.*, 2001, **84**, 675–677.
26. Uematsu, K., Ohsaka, S., Shinohara, N. and Okumiya, M., Grain-oriented microstructure of alumina ceramics made through the injection molding process. *J. Am. Ceram. Soc.*, 1997, **80**, 1313–1315.
27. Maca, K., Hadraba, H. and Cihlar, J., Study of sintering of ceramics by means of high-temperature dilatometry. *Ceramics-Silikáty*, 1998, **42**, 151–158.
28. Van Krevelen, D. W., *Properties of Polymers. Their Correlation with Chemical Structure; their Numerical Estimation and Prediction from Additive Group Contributions*. Elsevier Science Publishers, Amsterdam, 1990 pp. 71–241.